Structure and dielectric properties of $Bi_{5-x}La_xNb_3O_{15}$ ceramics

Zhiguo Yi · Yongxiang Li · Jiangtao Zeng · Qunbao Yang · Qingrui Yin

Abstract $Bi_{5-x}La_xNb_3O_{15}$ ($x=0$–1.25) ceramics prepared by conventional solid-state reaction were studied using X-ray diffraction (XRD), electron probe microanalysis (EPMA) and dielectric spectroscopy techniques. The XRD analysis indicated single phase solid solution of $Bi_{5-x}La_xNb_3O_{15}$ is formed for $x \leq 1.25$. EPMA showed good densification and homogeneous microstructures for the ceramics. With increasing x, the dielectric constant decreases monotonously and can vary from 258 to 158 at 300 kHz. The frequency dependence of dielectric constants indicated these ceramics are promising candidates for high frequency applications.

Keywords $Bi_{5-x}La_xNb_3O_{15}$ · Bismuth layer-structured ferroelectric · Solid solution · Microstructure

1 Introduction

Bismuth layer-structured compounds are an important family of ferroelectrics, which have great potential in ferroelectric, pyroelectric, piezoelectric and dielectric applications [1–6]. However, as the spontaneous polarization movements are restricted to a (b) plane of the unit cell (the

Z. Yi · Y. Li (✉) · J. Zeng · Q. Yang · Q. Yin
The State Key Lab of High Performance Ceramics and Superfine Microstructures, Shanghai Institute of Ceramics, Chinese Academy of Sciences,
Shanghai 200050, People's Republic of China
e-mail: yxli@mail.sic.ac.cn

Z. Yi
Postgraduate School, Chinese Academy of Sciences,
Beijing 100390, People's Republic of China

c-axis component can be neglected), the ferroelectric or piezoelectric property is much lower than that of PZT materials. Therefore, structural modifications are widely used to enhance their ferroelectric or piezoelectric properties and such efforts have been recently extended to the system of intergrowth bismuth layer-structured ferroelectrics (IBLSFs) [4–7].

The IBLSFs are usually made up of an intergrowth of one-half the unit cell of usual BLSF, and one half the unit cell of another BLSF along the c-axis, with the difference of the numbers of perovskite-like layers that sandwiched between $(Bi_2O_2)^{2+}$ layers equals unity ($m-n=1$). For example, the IBLSFs $Bi_5TiNbWO_{15}$ and $SrBi_8Ti_7O_{27}$ are made up of Bi_3TiNbO_9 ($m=2$) and Bi_2WO_6 ($n=1$), $SrBi_4Ti_4O_{15}$ ($m=4$) and $Bi_4Ti_3O_{12}$ ($n=3$) along each c-axis, respectively.

To this kind of natural superlattice structure, the structure modification has been carried out for $SrBi_8Ti_7O_{27}$ and $BaBi_8Ti_7O_{27}$ through La^{3+}, Sm^{3+}, and Nd^{3+} substitution for Bi^{3+} [7–10]. In these situations, generally, the sites and content of lanthanum have great influence on the dielectric and ferroelectric properties. In the present paper, $Bi_5Nb_3O_{15}$ ceramics are modified by La^{3+} substitution for Bi^{3+}, and the structure and the dielectric properties are investigated for such modified ceramics.

2 Experimental

$Bi_{5-x}La_xNb_3O_{15}$ ceramics ($x=0$, 0.25, 0.50, 0.75, 1.00, 1.25) were synthesized by a solid-state reaction process from the high purity Bi_2O_3 (99%), La_2O_3 (99.99%) and Nb_2O_5 (99.5%) raw powders. Firstly, the weighted powders were mixed by yttria stabilized zirconia (3Y-TZP) ball milling in

ethanol for 4 h, and then calcined at 850 °C in air for 7 h after drying. Secondly, these calcined powders were re-milled, dried, and polyvinyl alcohol was added before pressed into cylindrical compacts of 13 mm in diameter and 1 to 2 mm in thickness under uniaxial pressure. Finally, the compacts were sintered at 1100 to 1170 °C in air for 2 h to make dense ceramics. For XRD analysis, the sintered samples were crushed to fine powders and recorded using CuK_α radiation in a Rigaku D/max-2550V diffractometer. The microstructures were characterized by electron probe microanalysis (EPMA). The dielectric characters were carried out on Pt-pasted samples by a TH2818 impedance analyzer (Changzhou Tonghui Electronic Instrument Co. Ltd, China).

Fig. 2 The variation of lattice constants of $Bi_{5-x}La_xNb_3O_{15}$ samples

3 Results and discussion

The structure of $Bi_5Nb_3O_{15}$ is considered to be composed of a regular intergrowth of one half the unit cell of $Bi_2NbO_{5.5}$ and one half the unit cell of $Bi_3Nb_2O_{9.5}$ [11]. Figure 1 shows the XRD patterns of $Bi_{5-x}La_xNb_3O_{15}$ powders. The coincidence of diffraction peaks for the samples at various x values indicates that La^{3+} doping does not affect the crystal structure. Figure 2 shows the lattice parameters of the solid solution with different x. With the increase of La^{3+} doping content, there are two relatively apparent transitions occurred at $x=0.50$ and $x=1.25$. It is widely accepted that $(Bi_2O_2)^{2+}$ is a rigid layer and when substituting La^{3+} for Bi^{3+}, La^{3+} will preferentially enter A sites in perovskite-like layers [12]. However, for the compounds $Bi_{5-x}La_xNb_3O_{15}$, when $x>1.00$ the La^{3+} will enter into $(Bi_2O_2)^{2+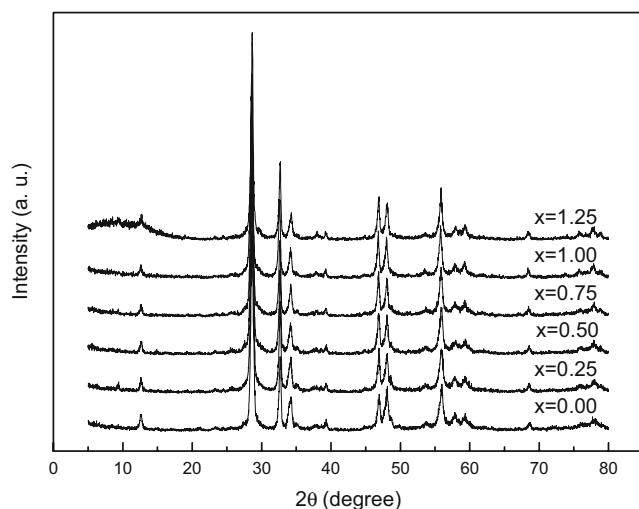}$ layers. So the lattice parameters variation with x implies the position variations for the substituting La^{3+}, i.e. when $x=0.50$, the Bi^{3+} in $(Bi_2O_2)^{2+}$ layers starts to be substituted. Furthermore, it suggests that A sites substituting increases c-axis whereas $(Bi_2O_2)^{2+}$ substituting decreases c-axis.

The dense ceramics based on $Bi_{5-x}La_xNb_3O_{15}$ can be obtained by sintering at temperatures ranging from 1100 to 1170 °C. Figure 3 shows the EPMA images of the as sintered surfaces of $Bi_{5-x}La_xNb_3O_{15}$ ceramics. No obvious pores or abnormal grains are observed, which confirm good densification and homogeneous microstructures.

La^{3+} substitution for Bi^{3+} significantly affects the dielectric properties of $Bi_5Nb_3O_{15}$ ceramics. Figure 4 shows changes in the dielectric constant and dielectric loss (at a frequency of 300 kHz) of $Bi_{5-x}La_xNb_3O_{15}$ ceramics as function of x. With increasing x, the dielectric constant decreases monotonously and can vary from 258 to 158 at 300 kHz, whereas the dielectric loss first decreases then increases. The decrease of dielectric constant is attributed to La^{3+} doping, since La^{3+} doping decreases the orthorhombic distortion of NbO_6 and thus reduces the ferroelectricity [13]. Figure 5 shows the dielectric constant and dielectric loss of $Bi_{5-x}La_xNb_3O_{15}$ ceramics as a function of frequency at room temperature. These dielectric ceramics indicate slight frequency dependence and subsequently they are promising candidates for high frequency applications.

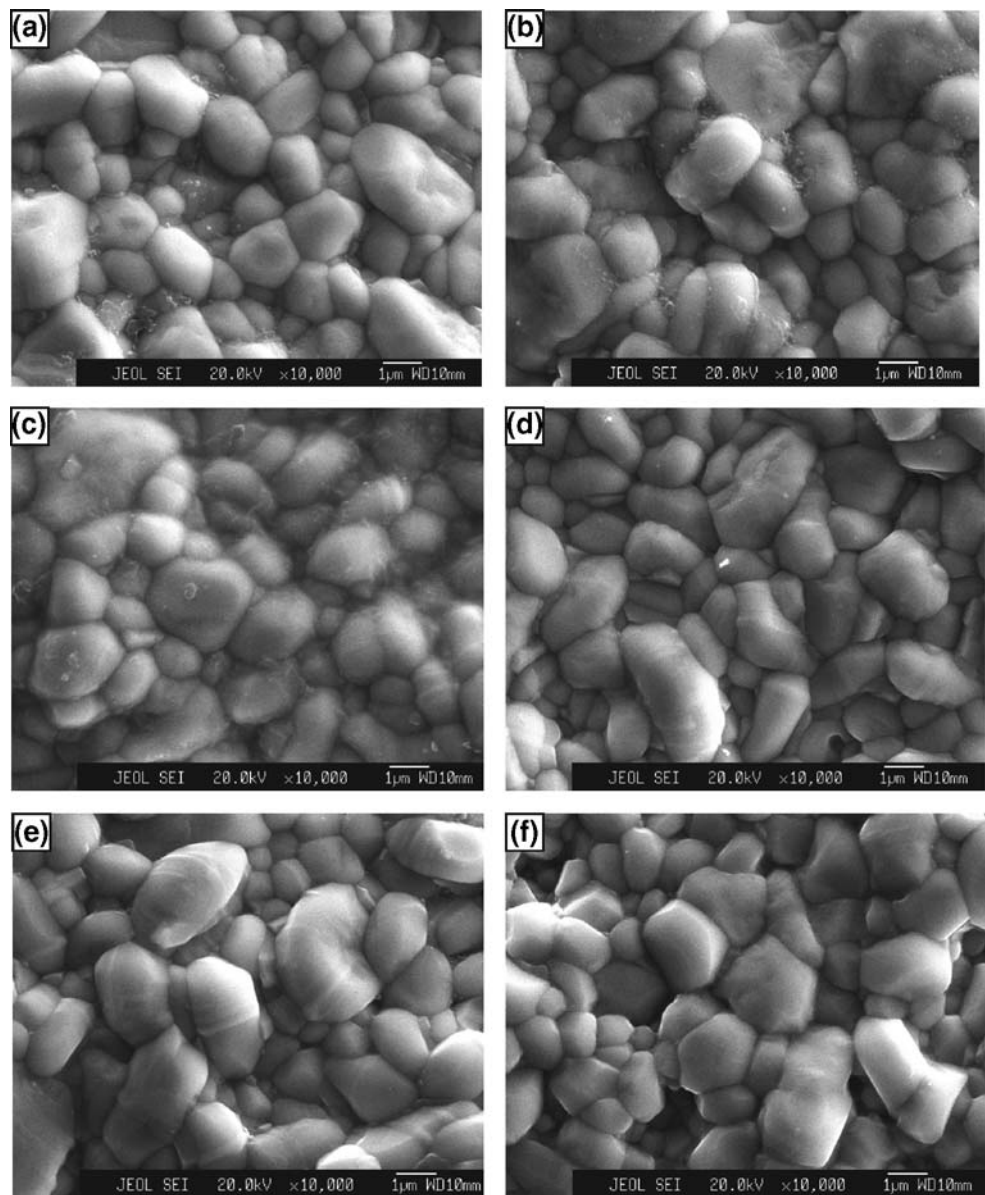Fig. 1 X-ray diffraction patterns of $Bi_{5-x}La_xNb_3O_{15}$ powders ($x=$ 0.00–1.25) at room temperature

4 Conclusion

Substitution of La^{3+} for Bi^{3+} significantly affects the structure and dielectric properties of $Bi_5Nb_3O_{15}$ ceramics.

Fig. 3 Electron probe micro-analysis images of as sintered surfaces of $Bi_{5-x}La_xNb_3O_{15}$ dense ceramics. (**a**) $x=$ 0.00 sintered at 1100 °C; (**b**) $x=0.25$ sintered at 1100 °C; (**c**) $x=0.50$ sintered at 1120 °C; (**d**) $x=0.75$ sintered at 1120 °C; (**e**) $x=1.00$ sintered at 1140 °C; (**f**) $x=1.25$ sintered at 1170 °C

Solid solution of $Bi_{5-x}La_xNb_3O_{15}$ ceramics was formed for $x\leq1.25$. EPMA showed dense, uniform and homogenous microstructure for all the ceramic specimens. With increasing x, the dielectric constant decreases monotonously, whereas dielectric loss first decreases then increases slightly. The frequency dependence of dielectric constants indicated these ceramics are promising candidates for high frequency applications.
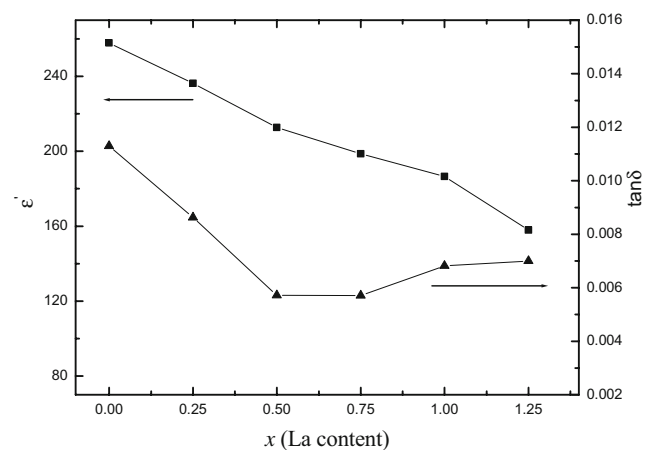
Fig. 4 The dielectric constant and dielectric loss (at 300 kHz) of $Bi_{5-x}La_xNb_3O_{15}$ ceramics as function of x

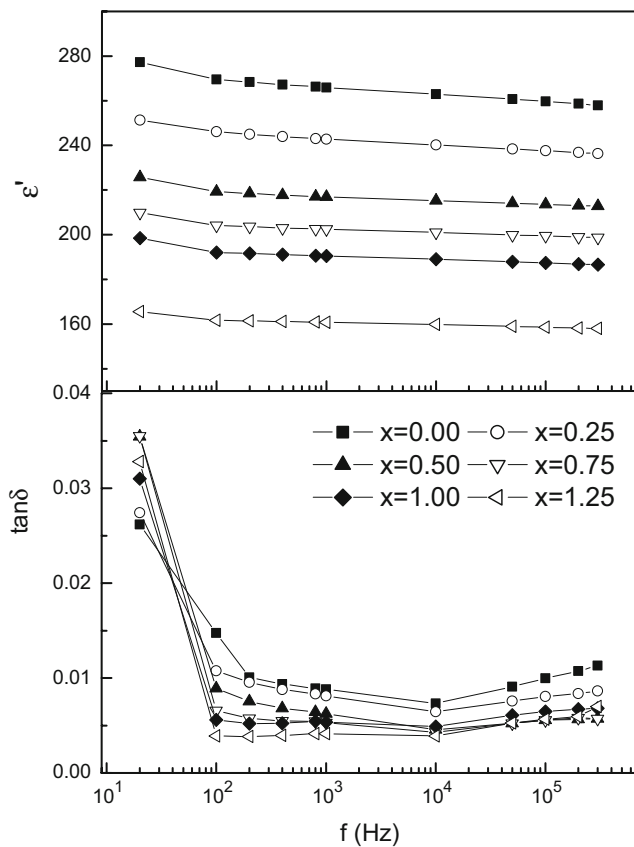**Fig. 5** The dielectric constant and dielectric loss of $Bi_{5-x}La_xNb_3O_{15}$ ceramics as a function of frequency, measured at room temperature

References

1. C.A. Paz de Araujo, L.D. McMillan, J.D. Cuchiaro, M.C. Scott, J. F. Scott, Nature **374**, 627 (1995)
2. B.H. Park, B.S. Kang, S.D. Bu, T.W. Noh, J. Lee, W. Jo, Nature **401**, 683 (1999)
3. Y. Noguchi, M. Miyayama, Appl. Phys. Lett. **78**, 1903 (2001)
4. Y. Noguchi, M. Miyayama, T. Kudo, Appl. Phys. Lett. **77**, 3639 (2000)
5. Y. Goshima, Y. Noguchi, M. Miyayama, Appl. Phys. Lett. **81**, 2226 (2002)
6. Z.G. Yi, Y.X. Li, Z.Y. Wen, S.R. Wang, J.T. Zeng, Q.R. Yin, Appl. Phys. Lett. **86**, 192906 (2005)
7. J. Zhu, X.B. Chen, W.P. Lu, X.Y. Mao, R. Hui, Appl. Phys. Lett. **83**, 1818 (2003)
8. X.M. Chen, R.Z. Hou, N.P. Jiang, J. Electroceramics **8**, 229 (2002)
9. R.Z. Hou, X.M. Chen, S.Y. Wu, Jpn. J. Appl. Phys. **42**, 5169 (2003)
10. R.Z. Hou, X.M. Chen, Mater. Res. Bull. **38**, 63 (2003)
11. T. Takenaka, K. Komura, K. Sakata, Jpn. J. Appl. Phys. **35**, 5080 (1996)
12. R.E. Newnham, R.W. Wolfe, J.F. Dorrian, Mater. Res. Bull. **6**, 1029 (1971)
13. M. Osada, M. Tada, M. Kakihana, T. Watanabe, H. Funakubo, Jpn. J. Appl. Phys. **40**, 5572 (2001)